BIOCHEMISTRY
including biophysical chemistry & molecular biology
Article

Biochemistry **2009,** *48,* 11273–11282 11273
DOI: 10.1021/bi901447j

A FRET-Based Method for Probing the Conformational Behavior of an Intrinsically Disordered Repeat Domain from *Bordetella pertussis* Adenylate Cyclase[†]

Géza R. Szilvay,[‡] Mark A. Blenner,[‡] Oren Shur,[‡] Donald M. Cropek,[§] and Scott Banta*[,‡]

[‡]*Department of Chemical Engineering, Columbia University, 500 West 120th Street, New York, New York 10027, and* [§]*U.S. Army Engineer Research and Development Center, Construction Engineering Research Laboratory, Champaign, Illinois 61822*

Received August 17, 2009; Revised Manuscript Received October 22, 2009

ABSTRACT: A better understanding of the conformational changes exhibited by intrinsically disordered proteins is necessary as we continue to unravel their myriad biological functions. In repeats in toxin (RTX) domains, calcium binding triggers the natively unstructured domain to adopt a β roll structure. Here we present an in vitro Förster resonance energy transfer (FRET)-based method for the investigation of the conformational behavior of an RTX domain from the *Bordetella pertussis* adenylate cyclase consisting of nine repeat units. Equilibrium and stopped-flow FRET between fluorescent proteins, attached to the termini of the domain, were measured in an analysis of the end-to-end distance changes in the RTX domain. The method was complemented with circular dichroism spectroscopy, tryptophan fluorescence, and bis-ANS dye binding. High ionic strength was observed to decrease the calcium affinity of the RTX domain. A truncation and single amino acid mutations yielded insights into the structural determinants of β roll formation. Mutating the conserved Asp residue in one of the nine repeats significantly reduced the affinity of the domains for calcium ions. Removal of the sequences flanking the repeat domain prevented folding, but replacing them with fluorescent proteins restored the conformational behavior, suggesting an entropic stabilization. The FRET-based method is a useful technique that complements other low-resolution techniques for investigating the dynamic conformational behavior of the RTX domain and other intrinsically disordered protein domains.

The exploration of intrinsically disordered proteins (IDPs)[1] has greatly broadened our view of protein structure−function relations. According to our current understanding, biologically relevant function can arise either from an unstructured (disordered), molten globule or from a structured protein conformation (*1*, *2*). Most known IDPs adopt a structured form upon interaction with a binding partner (*3*). The adenylate cyclase toxin (CyaA) protein from *Bordetella pertussis* (the etiologic agent of pertussis or "whooping cough") has an approximately 700-amino acid C-terminal part that is natively disordered in the absence of calcium ions (*4*). This segment has five domains that are each composed of tandemly repeated nonapeptides called repeats in toxins (RTX), named so since these motifs are often found in secreted bacterial toxins or virulence factors (*5*). Domains formed by tandemly arranged repeated RTX motifs are found in secreted proteins from Gram-negative bacteria, such as in hemolysins, lipases, zinc proteases, nodulation proteins, and cyclolysins (*6*−*10*). The RTX motifs have a general consensus sequence of GGXGXDXUX, where U denotes a large hydrophobic amino acid and X represents any amino acid. X-ray crystal structures of proteins containing RTX domains show that in the presence of calcium, the domain forms a right-handed β helical structure, the β roll, in which calcium ions are bound between turns (GGXGXD) that connect adjacent β strands (XUX) (*7*, *8*, *11*) (Figure 1A).

The C-terminal part of CyaA that contains the five RTX domains has been shown to bind calcium ions reversibly with low affinity (*12*, *13*). Thus, it has been suggested that in the bacterial cytosol, where calcium is scarce [nanomolar concentration (*14*)], the unstructured domain facilitates passage through the type I secretion system (*4*). After secretion into an extracellular medium with a millimolar calcium concentration, the RTX domains bind calcium and presumably form β roll structures that are characteristic of the RTX domains. This Ca^{2+}-dependent conformational change has been suggested to be an allosteric switch that causes a transformation of the CyaA into a biologically active form (*13*, *15*, *16*). In the active form, CyaA can bind to a target cell surface and form a pore with its hydrophobic domain. Subsequent translocation of CyaA into the cell causes uncontrolled cyclic AMP synthesis leading to cell death.

A general structural understanding of the behavior of RTX domains is emerging, although there are still features that need to be explained. The X-ray crystal or NMR structures of some proteins containing RTX domains in their calcium-bound state are available, but a structure of the CyaA RTX domains has not been reported. Understanding the conformational changes that take place in the RTX domains is important for elucidation of the mechanism of calcium-dependent secretion and activation of

[†]This work was funded by the Defense Threat Reduction Agency, the Academy of Finland (G.R.S.), and the Alfred Kordelin Foundation (G.R.S.).

*To whom correspondence should be addressed. Telephone: (212) 854-7531. Fax: (212) 854-3054. E-mail: sbanta@cheme.columbia.edu.

[1]Abbreviations: IDP, intrinsically disordered protein; CyaA, adenylate cyclase toxin; RTX, repeats in toxins; FRET, Förster resonance energy transfer; FP, fluorescent protein; CD, circular dichroism; MBP, maltose binding protein; bis-ANS, 4,4′-bis(1-anilinonaphthalene-8-sulfonate); FRET *E*, FRET efficiency; WLC, wormlike chain; EGTA, ethylene glycol tetraacetic acid; PDB, Protein Data Bank.

Published on Web 10/28/2009

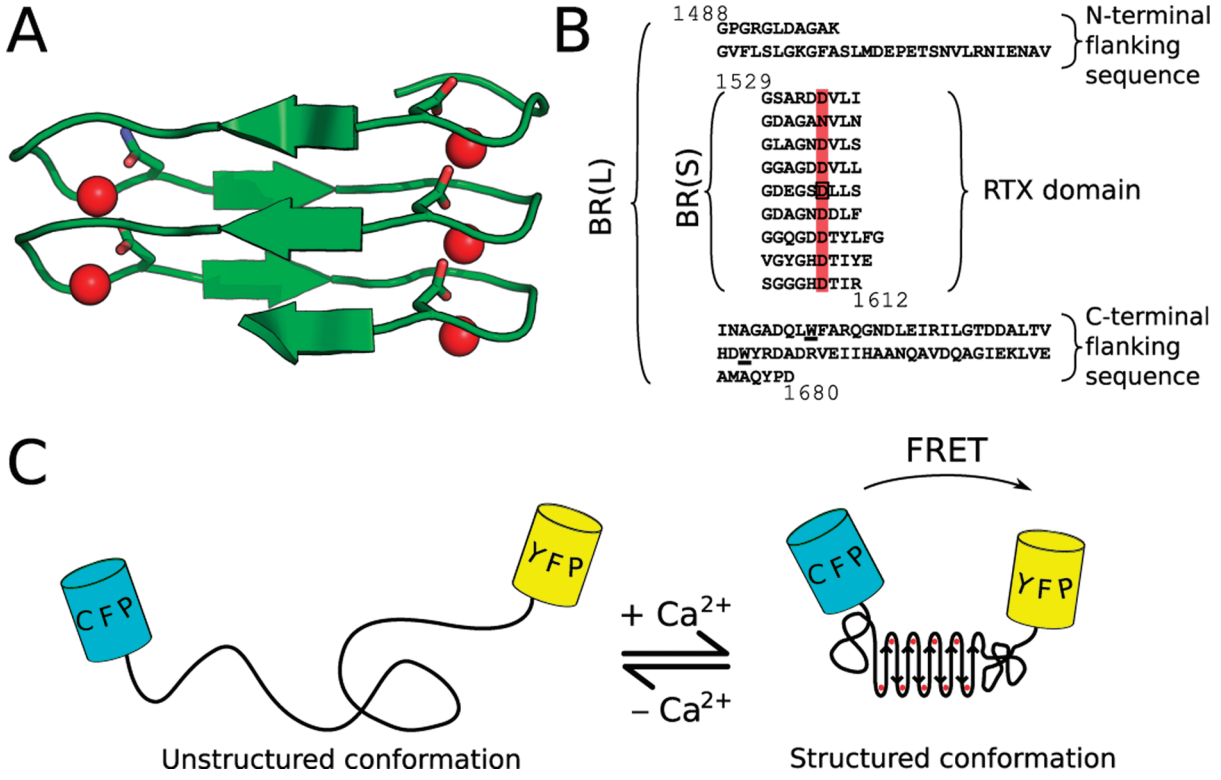

FIGURE 1: RTX domains and the genetically encoded FRET reporter. (A) β roll structure of the Ca^{2+}-bound state of an RTX domain from the *Serratia marcescens* serralysin enzyme (PDB entry 1SAT) (*49*). Ca^{2+} ions are shown as red spheres, and the side chains of the conserved Asp residues are highlighted. β strands, each formed by three amino acids, are shown as green arrows. Currently, there is no available protein structure of a CyaA β roll. However, on the basis of sequence homology, the RTX domains of CyaA are predicted to adopt similar β roll folds. (B) Sequence of the fifth RTX domain [named here BR(S), amino acids 1529−1612] and its flanking regions [BR(L), amino acids 1488−1680] of CyaA from *B. pertussis*. The conserved nonapeptide RTX domain is shown in the middle, and the conserved Asp residues involved in Ca^{2+} binding are highlighted (red shading). The flanking regions are indicated, and Trp residues (positions 1621 and 1645) are underlined. The Asp1570 residue mutated in this work is marked with a box. (C) Schematic image of the C-BR(L)-Y fusion protein construct showing the Ca^{2+}-dependent β roll structure formation that alters the distance between the FRET pair of CFP and YFP (not drawn to scale).

CyaA and other similar toxins. Furthermore, this will aid the development of efficient preventive and therapeutic strategies against *B. pertussis* infection.

The conformational behavior of IDPs or disordered peptides has been proposed to be of potential use in the development of protein switches (*17*−*20*). These proteins or peptides can function as stimulus-responsive elements that can modulate the properties of engineered systems, e.g., by changing cross-linking size in materials or attenuating protein function (*17*, *21*, *22*). Several research groups are working to improve our understanding of the function of control elements occurring in natural proteins and to utilize them as stimulus-responsive components in engineered systems.

To study the conformational changes of IDPs, and specifically the last RTX domain in CyaA, we have engineered a genetically encoded Förster resonance energy transfer (FRET) reporter (Figure 1B,C). In the fusion protein, the RTX domain is inserted between two fluorescent proteins (FPs) whose energy transfer efficiency depends on their relative separation distance. The method is a useful way to study the conformational changes in protein domains under various conditions. The results were compared with circular dichroism (CD) and fluorescence spectroscopy studies.

MATERIALS AND METHODS

Plasmid Constructs. To generate the FRET constructs, the genes for cyan fluorescent protein (CFP), an RTX domain, and yellow fluorescent protein (YFP) were assembled sequentially into the pET-20b(+) vector (Novagen, Gibbstown, NJ), upstream of a His_6 tag encoding segment. The details of the recombinant DNA work are available as Supporting Information. Also, the construction of CFP and YFP expression vectors pET/CFP and pET/YFP, respectively, nonfluorescent fusion protein C*-BR(S)-Y* expression vector pET/C*-CyaA$^{1488-1680}$-Y*, nonfluorescent CFP expression vector pET/CFP*, and the maltose binding protein−RTX domain fusions and site-directed mutagenesis are described in the Supporting Information.

Protein Expression and Purification. Proteins were expressed in *Escherichia coli* BL21(DE3) cells (Invitrogen, Carlsbad, CA). C-BR(L)-Y, C-BR(S)-Y, their mutants, and YFP control protein-expressing cells were induced at midlog growth phase with 0.04 mM isopropyl β-D-1-thiogalactopyranoside. Expression was continued for 16 h at 20 °C. Using these conditions, YFP and its fusion partners were expressed in soluble form, but expression at 37 °C for 4 h resulted in the accumulation of protein in inclusion bodies. CFP expression cultures were induced with 0.4 mM isopropyl β-D-1-thiogalactopyranoside at 37 °C for 4 h. The amount of expressed soluble CFP seemed to be approximately equal at 37 and 20 °C. Cells were harvested by centrifugation and resuspended in ice-cold 50 mM Tris-HCl buffer (pH 8) supplemented with 10 mM $CaCl_2$, 20 mM imidazole, and a protease inhibitor cocktail [Complete Mini, EDTA-free (Roche, Indianapolis, IN)] and lysed using an ultrasonicator tip. The target proteins were purified using HisTrap Ni-affinity chromatography (GE Healthcare, Piscataway, NJ),

concentrated using Amicon 15 ultrafiltration cartridges (Millipore, Billerica, MA), and subsequently applied to a 16/60 Superdex 200 preparative grade gel filtration chromatography column (GE Healthcare) equilibrated with 50 mM Tris-HCl buffer (pH 8) containing 200 mM sodium chloride. Fractions containing protein were pooled and exchanged into 50 mM Tris-HCl buffer (pH 8) by ultrafiltration. Samples analyzed by sodium dodecyl sulfate−polyacrylamide gel electrophoresis (SDS−PAGE) showed at least 95% purity. Protein concentrations were determined spectrophotometrically from CFP absorption using the published molar extinction coefficient (*23*). The resulting concentrations corresponded well to the values determined from the YFP absorption and its molar extinction coefficient (*23*).

The expression and purification of BR(L), BR(S), BR(L)-D/A, and BR(L)-D/P were conducted using the pMAL expression system (New England Biolabs, Ipswich, MA) according to the manufacturer's protocol. Briefly, the protein was expressed as a fusion to maltose binding protein (MBP); the clarified bacterial lysate was applied to an amylose column and washed, and the MBP fusion protein was eluted with maltose. Subsequently, enterokinase was used to cleave the MBP from its fusion partner. The proteins were finally purified from MBP and enterokinase by anion exchange chromatography on a HiPrep 16/10 Q FF column (GE Healthcare) and size exclusion chromatography on a HiLoad 16/60 Superdex 75 column (GE Healthcare). SDS−PAGE analysis showed at least 95% sample homogeneity.

Fluorescence Spectroscopy and Quantitation of FRET Efficiency. Fluorescence spectroscopy was performed using a SpectraMax M2 (Molecular Devices, Sunnyvale, CA) spectrophotometer. Tryptophan fluorescence was measured by excitation at 295 nm and emission at 340 nm. FRET analysis was accomplished by exciting the donor fluorophore at 420 nm and recording the emission spectrum. The FRET efficiency (FRET *E*) [the fraction of excitation energy transferred from the donor (CFP) to the acceptor (YFP)] was observed as the increase in acceptor emission at 527 nm and calculated using the method described by Clegg (*24*) and utilized earlier in protein−protein interactions (*25*). The method has several benefits as compared to the often used donor quenching method (*24*). Small amounts of free donor in the sample (such as from degraded fusion protein) do not affect the calculated FRET *E*. Furthermore, the method uses the directly excited acceptor fluorescence as an internal control for concentration, thus accounting for any variation in protein concentration across samples.

According to the method (*24*), the fluorescence contribution of the acceptor was extracted from the emission spectrum via subtraction of a normalized fluorescence spectrum of a donor-only sample from that of the measured sample. The resulting spectrum contains the acceptor fluorescence arising from FRET and directly excited acceptor. This spectrum was then divided by the fluorescence of the acceptor when excited directly at 490 nm, where only the acceptor is excited. The resulting fluorescence $(\text{ratio})_A$ can be described as follows

$$(\text{ratio})_A = \left[E\frac{\varepsilon^{CFP}(420)}{\varepsilon^{YFP}(490)} + \frac{\varepsilon^{YFP}(420)}{\varepsilon^{YFP}(490)}\right]\frac{\phi^{YFP}(\nu_1)}{\phi^{YFP}(\nu_2)} \quad (1)$$

where $\varepsilon(\lambda)$ denotes the extinction coefficients of CFP and YFP at wavelength λ (*24*) and $\phi(\nu)$ denotes the quantum yield at wavelength ν. As the same emission wavelength was used to measure both the FRET *E* and the fluorescence of the directly excited acceptor, the quantum yield ϕ^{YFP} ratio was unity. The term $\varepsilon^{CFP}(420)/\varepsilon^{YFP}(490)$ was measured to be 0.3518 and $\varepsilon^{YFP}(420)/\varepsilon^{YFP}(490)$ to be 0.0193. The apparent interchromophore distance *r* was calculated from the FRET efficiency using the equation

$$\text{FRET } E = \frac{1}{1+(r/R_0)^6} \quad (2)$$

where the published Förster distance R_0 of 4.9 nm (*26*) was used and assuming a random relative orientation of donor and acceptor (orientation factor K^2 value set to $^2/_3$).

Titrations were performed at a protein concentration of 1 μM with $CaCl_2$, NaCl, $(NH_4)_2SO_4$, or $MgCl_2$, in 50 mM Tris-HCl buffer (pH 8.0). Origin 8.0 (OriginLab, Northampton, MA) was used to fit the Hill model to the titration curve data and retrieve the best-fit values for the apparent K_D and Hill coefficients.

We measured the fluorescence of the dye 4,4′-bis(1-anilinonaphthalene-8-sulfonate) (bis-ANS) (Sigma, St. Louis, MO) at 1.6 μM in the presence of 250 nM protein with a Jasco J-815 spectrometer by exciting the sample at 390 nm and scanning the emission spectra from 420 to 600 nm.

Comparison of FRET-Derived Dimensions with Theoretical Polymer Models. The continuous wormlike chain (WLC) model was used to describe a random coil structure between the FPs (*27*). In this model, the average end-to-end distance of a polymer is described by rigid segments characterized by the persistence length l_p. The mean square end-to-end distance of a polymer spanning a contour length l_c is

$$\langle r^2\rangle = 2l_p l_c - 2{l_p}^2\left[1-\exp\left(\frac{-l_c}{l_p}\right)\right] \quad (3)$$

The contour length, l_c, for a polypeptide chain was defined as 0.38 nm per amino acid. In addition to the RTX inserts (195 or 86 amino acids, including a two-amino acid linker), 11 amino acids in CFP and three in YFP that link the FP terminus to structured parts of the FP were estimated to be unstructured on the basis of X-ray crystal structures (PDB entries 1CV7 and 1YFP). Furthermore, for the sake of simplicity, the chromophore−FP surface distances of 1.5 and 2.3 nm for CFP and YFP, respectively, were approximated as being flexible. Thus, the l_c between chromophores for C-BR(L)-Y and C-BR(S)-Y was estimated to be 83 and 42 nm, respectively. For the model of a self-avoiding walk of a freely jointed Gaussian chain formed by *N* links each having a length *a* of 0.38 nm ($l_c = aN$), the mean end-to-end distance was described as $r = aN^{3/5}$ (*28*).

Stopped-Flow FRET. Folding kinetics of C-BR(L)-Y were measured as the change in FRET acceptor fluorescence in time with a Jasco J-815 spectrometer equipped with a fluorescence monochromator (FMO-427S/15) (Jasco Inc., Easton, MD) and a stopped-flow apparatus (SFM-20) with a 2 mm light path cuvette (dead time of ~10 ms) (Bio-Logic, Claix, France). Samples were excited at 420 nm, and the emission of the acceptor was monitored at 527 nm. We measured the rates of calcium-induced fluorescence change by rapidly mixing 4 μM protein and 0−1 mM $CaCl_2$ in 50 mM Tris buffer (pH 8). We measured unfolding rates by rapidly mixing protein preincubated with 0−10 mM $CaCl_2$ and a 5−20-fold molar excess of ethylene glycol tetraacetic acid (EGTA). The EGTA concentrations used did not have an observed effect on the unfolding rates. Single-exponential curves were fit to the data using Origin 8 (OriginLab) to determine the values of the observed rate constants (k_{obs}).

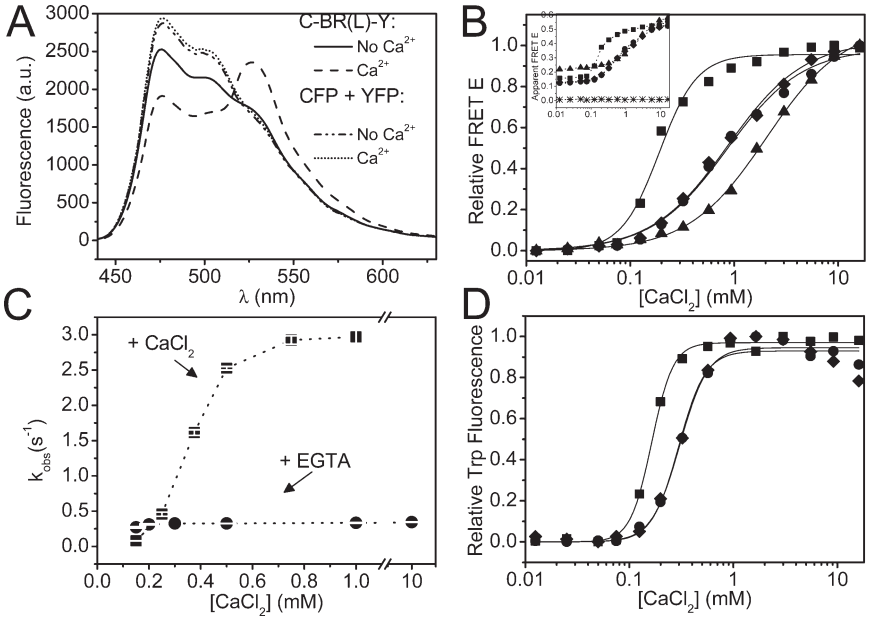

FIGURE 2: Calcium-induced conformational change as observed by a change in FRET *E* and Trp fluorescence. (A) Emission spectra of 1 μM C-BR(L)-Y in the absence (—) and presence (---) of 10 mM $CaCl_2$ when excited at 420 nm. An increase in FRET *E* was seen as a decrease in CFP fluorescence (475 nm) and an increase in YFP fluorescence (527 nm). Addition of $CaCl_2$ did not affect the emission spectra of a mixture of 1 μM CFP and 1 μM YFP [no $CaCl_2$ (-·-) and $CaCl_2$ added (···)]. (B) Dependence of FRET *E* on $CaCl_2$ concentration. C-BR(L)-Y (■), C-BR(S)-Y (▲), and the mutants C-BR(L)-Y-D/A (●) and C-BR(L)-Y-D/P (◆) shown as a relative change in FRET *E*. The data with apparent FRET *E* values are shown in the inset. The mixture of 1 μM CFP and 1 μM YFP had no change in calculated FRET *E* as a function of $CaCl_2$ (inset, ∗). The lines are best fits of the Hill equation as described in Materials and Methods. (C) Rapid kinetics of C-BR(L)-Y folding (■) and unfolding (●) at the indicated $CaCl_2$ concentrations was measured using FRET as described in Materials and Methods. Error bars represent standard errors ($N \geq 3$). Representative fluorescence time course traces are shown in Figure S1 of the Supporting Information. (D) Relative tryptophan fluorescence upon addition of $CaCl_2$ in C-BR(L)-Y (■) and mutants C-BR(L)-Y-D/A (●) and C-BR(L)-Y-D/P (◆). The Hill equation was fitted to the data (lines).

Circular Dichroism Spectroscopy. Far-UV circular dichroism (CD) spectroscopy was performed with a Jasco J-815 CD spectrometer equipped with a Peltier temperature control in a 0.01 cm quartz cuvette. Samples were scanned in 50 mM Tris-HCl buffer (pH 8) from 250 to 190 nm in continuous mode, with a scan speed of 50 nm/min and a response time of 2 s, and by accumulating five scans at 25 °C. Secondary structure contents were estimated using CDPro (*29*).

RESULTS

The β roll domain chosen for this study was the fifth RTX domain block (residues 1488−1680) of CyaA from *B. pertussis* (Uniprot entry P15318). This sequence includes the N- and C-terminal non-RTX sequences that flank the core nine-repeat RTX domain and were previously shown to be required for the calcium-responsive conformational change (*13*). Residues 1488−1528 and 1613−1680, upstream and downstream of the RTX domain, respectively, are here termed flanking sequences (Figure 1B). The protein was termed $CyaA^{1488-1680}$ by Bauche et al. (*13*) and is here termed BR(L) for the sake of simplicity ("L" for long). The fusion protein in which BR(L) was inserted between the FPs was named C-BR(L)-Y, where C and Y refer to CFP and YFP, respectively. The core RTX domain sequence without the flanking sequences comprising amino acids 1529−1612 was similarly inserted between the FPs, yielding C-BR(S)-Y ("S" for short). All used RTX domain constructs used in this study are summarized in Table S1 (Supporting Information).

Calcium-Free Conformation of the CyaA RTX Domain. FRET taking place between the FPs was observed as a reduction in CFP (donor) fluorescence and increase in YFP (acceptor) fluorescence when exciting the donor at 420 nm (Figure 2A). In the absence of $CaCl_2$, the C-BR(L)-Y sample had a FRET *E* of 0.15 ± 0.03 [mean ± standard deviation (SD); $N = 3$] that corresponds to an average inter-FP distance of ~6.6 ± 0.3 nm, when assuming a random orientation of the donor and acceptor. Similarly, the initial FRET *E* for the shorter RTX domain, C-BR(S)-Y, was 0.22 ± 0.01, corresponding to an average inter-FP distance of 6.1 ± 0.1 nm. As expected, an equimolar mixture of free CFP and YFP had a very low FRET *E* value of 0.012 ± 0.001 (Figure 2A and Figure 2B, inset).

To improve our understanding of the calcium-free conformation, the inter-FP distances obtained by FRET were compared with the dimensions of theoretical flexible polymers. According to the Gaussian self-avoiding walk model, an ideally flexible chain with a length corresponding to that of BR(L) and BR(S) (and including all linker sequences as described in Materials and Methods) has an average length of 9.6 and 6.4 nm, respectively (Table 1). The FRET distance measurements for the C-BR(S)-Y insert (6.1 nm) agreed well with a polypeptide that behaves as a Gaussian chain (6.4 nm). The C-BR(L)-Y insert, however, has more compact dimensions (6.6 nm) than a corresponding Gaussian chain (9.6 nm).

The WLC model was then used to describe the flexibility of the RTX domains. This model describes the conformation distribution of a semiflexible polymer where chain segment direction has a persistent memory characterized by the persistence length, l_p. The persistence length values for C-BR(L)-Y and C-BR(S)-Y were calculated using eq 3 and the apparent FP separation distances obtained by FRET and were determined to be 0.26 and 0.45 nm, respectively (Table 1). The value for l_p has previously been determined to be approximately 0.5−0.7 nm for large IDPs, 0.4−0.45 nm for flexible polypeptide linkers, and 0.3 nm for protein loop structures (*27*, *30*, *31*). The l_p value for C-BR(S)-Y thus corresponds to a flexible or disordered WLC and

Table 1: Interchromophore Distances Determined by FRET and Comparison with Theoretical Polymer Models

				FRET measurements			
				Ca^{2+}-free state		Ca^{2+}-bound state	
RTX domain	no. of amino acids in the RTX domain	interchromophore l_c (nm)[a]	$\langle r \rangle_{Gaussian}$ (nm)[b]	r_{FRET} (nm)[c]	l_{pWLC} (nm)[d]	r_{FRET} (nm)[c]	l_{pWLC} (nm)[d]
C-BR(L)-Y	193	83.2	9.6	6.6 ± 0.3	0.26	4.7 ± 0.3	N/A (0.14)[e]
C-BR(S)-Y	84	41.8	6.4	6.1 ± 0.1	0.45	4.7 ± 0.2	N/A (0.27)[e]

[a]Contour length (l_c) between the chromophores of the FPs, calculated as described in Materials and Methods. [b]Average end-to-end distance of a theoretical Gaussian chain with contour length l_c. [c]FRET data shown as means ± the standard deviation ($N = 3$). [d]Persistence length l_p was calculated using the WLC model in which the interchromophore distance was obtained from FRET measurements as described in Materials and Methods. [e]The WLC model is not applicable as such to the structured state because the l_c of a structured protein is defined by the structure and not by the extended chain length. The values given in parentheses are calculated using the l_c of a fully extended chain solely to indicate that the values are smaller than those of the calcium-free conformation.

that of C-BR(L)-Y to a comparably more structured conformation.

Calcium-Induced FRET Change. The addition of 10 mM $CaCl_2$ to C-BR(L)-Y caused a rapid reduction in the CFP fluorescence and an increase in the YFP fluorescence as shown in Figure 2A. The calculated FRET E in 10 mM $CaCl_2$ was approximately 0.57 ± 0.09. This calcium-dependent change in FRET E from 0.15 to 0.57 was attributed to a change in RTX domain end-to-end distance and thus folding of the RTX domain. The fluorescence emission spectrum of the control sample containing a 1:1 ratio of free CFP and YFP did not change upon addition of $CaCl_2$ (Figure 2A,B). The calcium-induced FRET E for C-BR(S)-Y increased from 0.22 ± 0.01 to ~0.56 ± 0.06 (Figure 2B), and thus, both RTX domains reached the same FRET E values that correspond to apparent average FP separations of 4.7 ± 0.3 and 4.7 ± 0.2 nm for C-BR(L)-Y and C-BR(S)-Y, respectively (Table 1).

To compare the FRET-derived dimensions of the calcium-bound state with the size of a theoretical β roll structure, the rough dimensions of potential β roll structures were estimated from available X-ray crystal structures (see the Supporting Information). The total interchromophore distances for a theoretical β roll structure formed by all amino acids between the FPs in C-BR(L)-Y (193-amino acid RTX insert) and in C-BR(S)-Y (84-amino acid RTX insert) would be roughly 7.5 and 4.8 nm, respectively. Thus, the FRET-derived apparent distance value for calcium-bound C-BR(S)-Y (4.7 nm) corresponds well to the size of the theoretical inter-FP distance when the insert assumes an all-β roll structure. As the calcium-bound structure of C-BR(L)-Y had very similar FRET dimensions (4.7 nm) but possesses the additional non-RTX flanking regions, these flanking regions possibly adopt a compact conformation that places the termini (and thus the FPs) close to the ends of the β roll domain. However, it is also possible that folding brings the two FPs into the proximity of each other so that they can interact in a similar way both in C-BR(L)-Y and in C-BR(S)-Y.

Calcium Binding Affinity and Kinetics As Measured by FRET. The Ca^{2+}-induced folding of C-BR(L)-Y, its mutants, and C-BR(S)-Y was studied by equilibrium titration experiments (Figure 2B). The Hill model was fitted to the data using nonlinear regression, and the obtained parameters are summarized in Table 2. The calcium-dependent FRET E change in C-BR(L)-Y was clearly sigmoidal in shape, having a Hill coefficient of 2.4 and an apparent K_D of 190 μM for Ca^{2+}. The data show that the affinity for Ca^{2+} is relatively low and folding is cooperative. Calcium titrations with C-BR(S)-Y showed that this protein had an even lower affinity, having an apparent K_D of 2.0 mM for calcium. Moreover, C-BR(S)-Y was almost noncooperative with a Hill coefficient of 1.16.

Table 2: Apparent Dissociation Constants and Hill Coefficients of RTX Domains for Ca^{2+} Binding As Measured by FRET and Trp Fluorescence[a]

	FRET		Trp fluorescence	
RTX domain	apparent K_D (μM)	Hill coefficient	apparent K_D (μM)	Hill coefficient
C-BR(L)-Y	190 ± 10	2.40 ± 0.29	160 ± 3	4.23 ± 0.30
C-BR(L)-Y-D/A	860 ± 60	1.19 ± 0.07	290 ± 20	3.39 ± 0.68
C-BR(L)-Y-D/P	850 ± 70	1.20 ± 0.09	310 ± 10	3.23 ± 0.41
C-BR(S)-Y	2040 ± 110	1.16 ± 0.04	N/A[b]	N/A[b]

[a]Determined in 50 mM Tris-HCl buffer at pH 8.0 and 25 °C. Values (mean ± standard error of the mean) were obtained from best fits of the Hill equation to the data. [b]C-BR(S)-Y lacks Trp residues.

To investigate the role of the Asp residues in the CyaA RTX domain conformational change, the Asp residue in the fifth RTX nonapeptide repeat was mutated to an Ala or a Pro residue, resulting in C-BR(L)-Y-D/A and C-BR(L)-Y-D/P. Both mutations significantly reduced the calcium affinity of the domain to ~850 μM (pairwise Student's t test; $p < 0.05$) (Figure 2B and Table 2). Furthermore, the Hill coefficients of both mutants were ~1.2, indicating an almost noncooperative calcium binding. The mutants and wild-type constructs reached approximately the same FRET E value at 10 mM Ca^{2+} (Figure 2B, inset).

To gain insight into the folding rates of the RTX domains, the fast kinetics of the FRET change of C-BR(L)-Y were followed using stopped-flow fluorescence spectroscopy. Empirically, the fluorescence change rate was a monoexponential process as the fluorescence traces were well fit by single-exponential functions (Figure S1, Supporting Information). A plot of the observed rate constant of the conformational change as a function of calcium concentration has a sigmoidal shape, suggesting that the folding is a multistep reaction that cannot be modeled with simple bimolecular rate equations (Figure 2C). The unfolding of the calcium-bound RTX under calcium-free conditions (EGTA as a Ca^{2+} sink) is a unimolecular process that occurred at a constant rate k_{off} of 0.33 s^{-1} over the studied calcium concentration range. Via application of the apparent K_D for calcium binding of 190 μM, an apparent association rate constant (k_{on}) of 1740 s^{-1} M^{-1} can be calculated (where $K_D = k_{off}/k_{on}$). As this is an apparent rate constant, however, it should be taken only as an overall value for the ensemble of the individual binding sites. As a whole, the preliminary kinetic results presented here indicate that the FRET method can potentially be applied to study the β roll folding mechanism in detail.

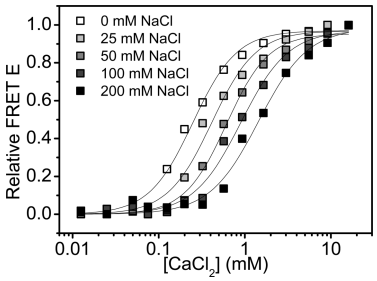

FIGURE 3: Effect of ionic strength on C-BR(L)-Y Ca^{2+} binding. Ca^{2+}-induced change to FRET *E* in buffer supplemented with 0−200 mM NaCl. The lines are best fits to the data with K_D values of 0.2, 0.4, 0.6, 0.9, and 1.4 mM.

Calcium-Induced Changes in Trp Fluorescence. The fluorescence of the Trp amino acid side chain is sensitive to the polarity of its local environment, and thus, Trp fluorescence can be used to study structural changes in proteins that take place near Trp residues. The BR(L) domain has two Trp residues in its C-terminal flanking sequence (see Figure 1B) that upon conformation change undergo increases in fluorescence intensity. Because of the linear nature of the β roll structure, the FRET and Trp fluorescence methods will report conformational changes of different parts of the protein. While the FRET measurements probe the average conformation of the whole protein, the Trp fluorescence emphasizes the C-terminal part of the protein. A combination of the two methods is very valuable as variation in the calcium binding properties along the length of the protein can be discerned.

In $CaCl_2$ titration experiments with C-BR(L)-Y, a sigmoidal increase in the Trp fluorescence was observed and an apparent K_D of 160 μM and Hill coefficient of 4.2 were obtained (Figure 2D and Table 2). The curve for C-BR(L)-Y was found to be very similar to the curve obtained with the FRET method (Figure 2B). The calcium affinities of the Ala and Pro mutants were lower than that of the wild type. However, the maximum change in Trp fluorescence was not affected by the mutations. The dissociation constants and Hill coefficients determined using both Trp fluorescence and FRET are compared in Table 2. The BR(S) protein does not contain any Trp residues as they are present only in the C-terminal flanking region, and thus, there was no change in Trp fluorescence upon calcium addition (data not shown).

RTX Conformational Changes in Different Environments. The Ca^{2+}-dependent FRET *E* change of C-BR(L)-Y was studied in various NaCl concentrations to explore the effect of ionic strength on the conformational change. The resulting calcium titration curves showed that with an increasing ionic strength, more $CaCl_2$ was needed to elicit the FRET response (Figure 3). The apparent dissociation constants increased as a function of ionic strength, from 0.19 mM in the absence of NaCl to 1.4 mM at 200 mM NaCl. The same ionic strength effect was also observed in Trp fluorescence measurements (data not shown).

Titrations were also performed with NaCl, $(NH_4)_2SO_4$, and $MgCl_2$ to explore the effect of different salts on C-BR(L)-Y conformation (Figure S2, Supporting Information). None of the tested salts affected the FRET *E* of equimolar mixtures of CFP and YFP. The FRET *E* and Trp fluorescence of C-BR(L)-Y increased only slightly as a function of ionic strength when titrated with NaCl or $(NH_4)_2SO_4$ (Figure S2A,B). The stronger hydrophobic interactions at high salt concentrations may cause

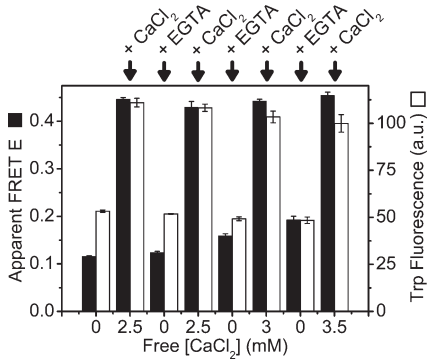

FIGURE 4: Reversibility of the C-BR(L)-Y conformational change. The Ca^{2+}-induced increase in FRET *E* (black) and Trp fluorescence (white) is reversed with EGTA. Repeated conformational changes were induced in the same sample by sequential additions of $CaCl_2$ and EGTA. The indicated concentrations are calculated as the free $CaCl_2$ concentration of each measurement. Error bars represent the standard deviation of individual experiments ($N = 3$).

C-BR(L)-Y to adopt a slightly more compact unfolded state conformation.

Titration with $MgCl_2$ caused an increase in FRET at high $MgCl_2$ concentrations; however, the apparent affinity for $MgCl_2$ was approximately 40-fold weaker compared to that for $CaCl_2$ (Figure S2A, Supporting Information). Trp fluorescence was not increased by the addition of $MgCl_2$ (Figure S2B, Supporting Information), and moreover, the Ca^{2+} titration Trp fluorescence curve was not affected by the presence of magnesium (data not shown). The effect of $MgCl_2$ on the FRET curve was identical with all tested proteins [C-BR(L)-Y, C-BR(S)-Y, and C-BR(L)-Y-D/A], demonstrating that the Mg^{2+}-induced FRET *E* increase is independent of the sequence between FPs. Furthermore, Mg^{2+} did not cause a change in the studied RTX domain CD spectra as discussed below. Thus, it is likely that $MgCl_2$ at high concentrations can cause a decrease in inter-FP distance by FP association or eliciting an alternative RTX conformation.

Reversibility of the Calcium-Induced Conformational Change. The chelating agent EGTA was able to reverse the calcium-induced increase in FRET *E* and Trp fluorescence in C-BR(L)-Y. Furthermore, by sequential additions of $CaCl_2$ and EGTA, the unstructured−folded transition could be observed at least four times (Figure 4). In the later rounds, the FRET *E* and Trp fluorescence values were likely affected by the accumulating ionic strength. As suggested by the NaCl titration experiments (Figure S2A,B), the high ionic strength present toward the end of the experiment can cause small changes in protein conformation.

Calcium-Induced Conformational Changes Observed via CD Spectroscopy. Conformational changes in RTX domains flanked with FPs could not be reliably studied with CD because the FPs, which are rich in β sheets, exhibited a dominating contribution to the CD spectrum. Therefore, CD spectroscopy was performed only on nonfused RTX domains lacking the FPs.

The addition of 10 mM $CaCl_2$ to the RTX domain BR(L) caused a significant change in the CD spectrum corresponding to a 7% increase in β sheet content (Figure 5). Addition of Ca^{2+} to the BR(S) protein did not change the CD spectrum, as has been previously reported (*13*). The CD spectra of the mutants BR(L)-D/A and BR(L)-D/P in the absence of Ca^{2+} were very similar to the spectrum of the wild-type protein. Upon addition of $CaCl_2$, a qualitative change in the CD spectrum was observed. However, upon deconvolution of the spectra, no significant secondary structure changes were observed. Addition of up to 10 mM

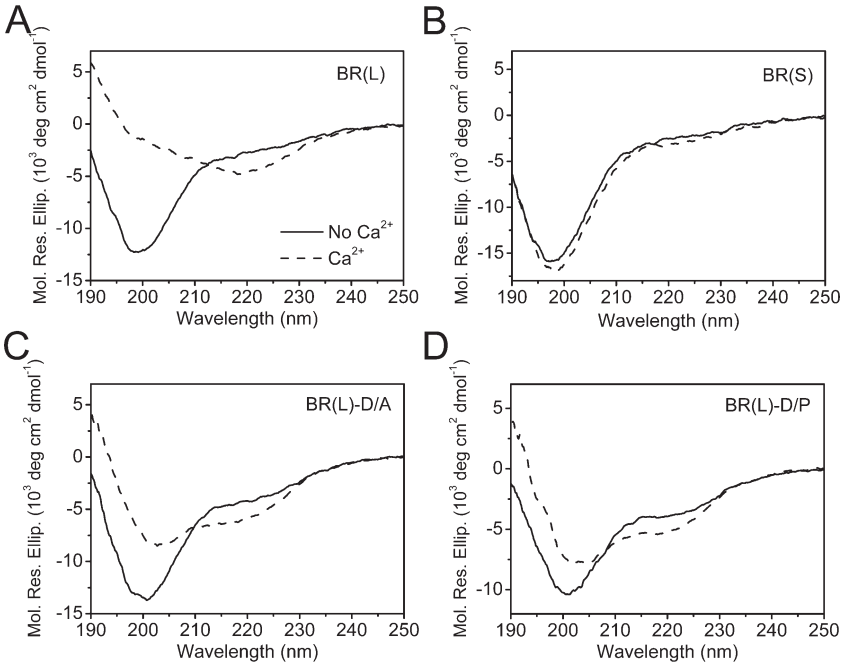

FIGURE 5: CD spectra of RTX domains in the presence (---) and absence (—) of $CaCl_2$. $CaCl_2$ induces a conformational change in BR(L) (A) but not in BR(S) (B). The mutants BR(L)-D/A (C) and BR(L)-D/P (D) exhibit an intermediate response to $CaCl_2$.

$MgCl_2$ or NaCl did not change the CD spectra of any of the RTX domains (data not shown).

Calcium-Induced Conformational Changes Observed by bis-ANS Fluorescence. On the basis of the FRET experiments, the C-BR(S)-Y conformation was calcium responsive but CD spectroscopy showed that the BR(S) conformation was not. Because of the lack of Trp residues in the uncapped variant BR(S), it was not possible to follow Trp fluorescence and the presence of the FPs in C-BR(S)-Y hindered CD spectroscopy experiments as discussed above. Thus, an orthogonal method for studying the conformational changes in the C-BR(S)-Y protein was desired to complement the FRET measurements. The fluorescent dye bis-ANS is often used as a reporter for changes in protein conformation as its fluorescence properties change upon binding to extended hydrophobic patches. As the fluorescence of the FPs interfered with bis-ANS fluorescence spectroscopy, a nonfluorescent mutant of C-BR(S)-Y, C*-BR(S)-Y*, was generated in which an essential Gly residue involved in the chromophore maturation was mutated to a Ser residue in both FPs (*32*) (see the Supporting Information).

The binding of bis-ANS to the nonfluorescent proteins C*-BR(S)-Y*, CFP*, and BR(S) was assessed in the presence and absence of $CaCl_2$ (Figure 6). Addition of 10 mM $CaCl_2$ to the nonfluorescent C*-BR(S)-Y* resulted in a 3.2-fold increase in the maximum fluorescence of bis-ANS, accompanied by a peak shift from 495 to 475 nm, indicative of a conformational change (Figure 6). NaCl at 10 mM had no significant effect on the bis-ANS fluorescence. Consistent with the CD measurements, addition of $CaCl_2$ to BR(S) caused an only 1.2-fold increase in bis-ANS fluorescence, indicating a lack of conformational change. In a control sample with 2 molar equiv of nonfluorescent CFP*, only a small fluorescence increase of 1.7-fold was observed with no change in peak wavelength.

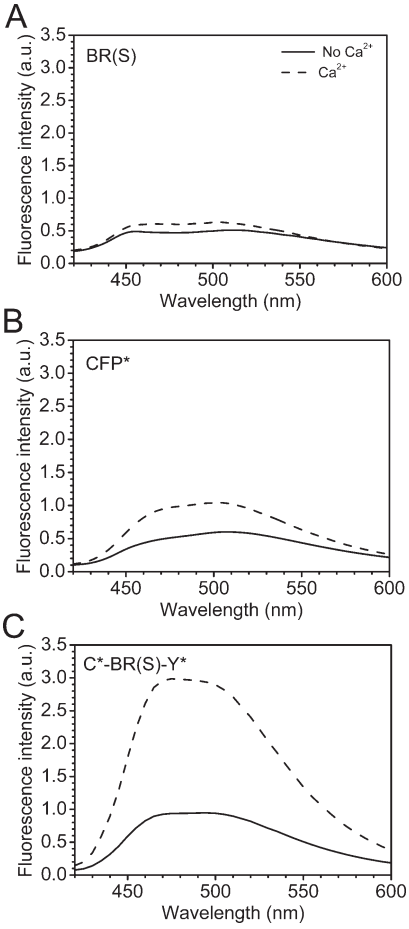

FIGURE 6: Calcium-induced changes in binding of bis-ANS to BR(S) (A), CFP* (B), and nonfluorescent C*-BR(S)-Y* (C). bis-ANS fluorescence spectra are shown in the absence (—) and presence (---) of 10 mM $CaCl_2$. The data for 2 molar equiv of CFP* are shown in panel B.

DISCUSSION

Design of the FRET-Based Conformational Change Reporter. FRET is a convenient and well-known method for the study of changes in distances between molecules or between parts of molecules (*33*), and thus, it has also been termed the

"spectroscopic ruler" (*34*). Using a suitable energy transfer donor and acceptor chromophore pair, the FRET efficiency (FRET *E*) depends on the donor−acceptor distance and relative orientation. To study the conformational changes in RTX domains, we engineered a genetically encoded FRET reporter that utilizes the distance-dependent changes in energy transfer from CFP to YFP. In the fusion protein, the studied RTX domains were sandwiched between the two FPs (Figure 1C) (*35*). Similar FRET constructs have previously been used to report the conformational changes in structured proteins, often with the goal of engineering intracellular sensors (*35*−*38*). The conformational ensemble of disordered proteins has been examined with FRET between FPs (*30*), and chemically linked small-molecule fluorophores have been used to study conformational changes in IDPs (*39*). This study shows that the genetically encoded FRET reporter system is a suitable method for the study of IDPs and their ligand-induced conformational changes. The advantages of this method over other low-resolution structural methods such as CD spectroscopy are that other components in the sample such as other proteins, buffer components, or impurities do not complicate the measurements. Furthermore, no chemical fluorophore labeling is necessary, and the measurements are relatively straightforward.

The FRET-based reporter can be used to study the conformations and structural dynamics of a CyaA RTX domain by measuring the apparent distance between the flanking FPs (Figure 1C). The studied RTX domain is predicted to form a calcium-binding β roll-like structure based on its high degree of sequence homology with known β roll-forming domains. Binding of Ca^{2+} ions and the Ca^{2+}-induced increase in β sheet content strongly support the structural prediction. Using the genetically encoded FRET constructs, we were able to explore the calcium-free and calcium-bound conformations and, furthermore, study the structural and environmental factors affecting the conformational change dynamics.

Unstructured Conformations of the RTX Domains. In the absence of calcium, the FRET-derived average interchromophore distance of C-BR(L)-Y was smaller than if the protein behaved as an ideal Gaussian chain-like polymer. Furthermore, the WLC model predicted that the persistence length was shorter than what is typical for IDPs, suggesting that some residual structure is present in this sequence. Also, the calcium-free conformation of BR(L) has been previously shown to possess residual structure as addition of denaturant was required for complete unfolding (*13*). C-BR(S)-Y, however, had a conformation that corresponded to a polymer behaving like a Gaussian flexible chain. Moreover, the WLC model predicted a persistence length that is typical for IDPs. The finding suggests that the conserved RTX sequence, BR(S), is mostly unstructured in the absence of calcium and the protein parts flanking this core sequence [found in BR(L)] have at least some residual structure. Recently, it has been shown that the ~700-amino acid C-terminal half of CyaA is unstructured in the absence of calcium (*4*). Our results show that there is variation in the extent of structure along the CyaA C-terminal part in the absence of Ca^{2+}. The studied fifth RTX domain has a high local concentration of negative charge (−12 in 84 residues) at physiological pH, mostly due to a high number of Asp residues, which probably cause electrostatic repulsion along the chain and perhaps effectively keep the domain unstructured (*40*).

Calcium-Induced Conformational Change in C-BR(L)-Y. Addition of Ca^{2+} ions to the unfolded RTX domain causes the equilibrium to shift toward the folded β roll state. When Ca^{2+} ions bind to the RTX domain, they can compensate for the negative charge and thus enable folding into the β roll conformation. The Ca^{2+} ions are an important structural part of the β roll as the polypeptide chain folds around the cations. The structure is also stabilized by hydrogen bonding in the β sheets and by hydrophobic interactions between the two β sheets (Figure 1A). Introducing calcium into C-BR(L)-Y causes a fast conformational change as observed by a decrease in the average FP distance using FRET and increase in Trp fluorescence (Figure 2). Correspondingly, a conformational change and an increase in β sheet content were observed with CD spectroscopy in BR(L) (Figure 5). Our data are consistent with a previous related study in which the conformational change in BR(L) was studied using CD, Trp fluorescence, and limited proteolysis (*13*).

Role of the Natural and Artificial Flanking Groups in β Roll Conformational Change. The importance of the flanking sequences for the RTX folding has previously been shown in CyaA (*13*). Consistent with previous reports, our studies using CD spectroscopy showed that the sequences flanking the RTX domain in BR(L) were necessary for a Ca^{2+}-induced conformational change as the BR(S) lacking those sequences was not responsive to Ca^{2+} (Figure 5). Surprisingly, when the RTX domain was studied with FRET using the C-BR(S)-Y construct, a significant calcium-induced conformational change was observed that resulted in approximately the same FRET *E* value as in C-BR(L)-Y (Figure 2B). The affinity and cooperativity for Ca^{2+} binding were, however, reduced compared to those of C-BR(L)-Y. Also, a conformational change was seen in C*-BR(S)-Y*, but not in BR(S), in bis-ANS binding experiments (Figure 6). Taken together, the results indicate that the FPs at both termini are able to restore the Ca^{2+}-dependent β roll structure formation ability of BR(S), though a higher Ca^{2+} concentration is needed. These natural end caps do not seem to have a specific role in formation of the β roll structure but may act as passive structural caps. It is possible that the large FP end caps reduce the entropy of the unfolded state and thus, in the presence of calcium, drive the equilibrium toward the folded state. In the folded state, the caps can potentially prevent fraying by providing interactions at the β roll ends and, moreover, shield the hydrophobic core.

The need for capping groups may be a general requirement for repeat proteins. Engineered caps have been designed for some repeat proteins based on their natural caps (*41*−*43*), but the possibility for nonrelated protein domains to act as artificial caps in repeat proteins has not been addressed previously. It remains to be seen if non-native capping groups can also be employed in other repeat proteins and, conversely, if proteins other than the FPs used here can function as capping groups. Further structural studies of the roles of the caps should provide insight into how the allosteric calcium-binding signal is translated through RTX folding to the rest of the protein.

Protein domains are known to be able to affect the folding of their fusion partners (*44*). Thus, it seems that the FP-based FRET method is particularly suitable for the study of protein fragments as the fragments are in a more nativelike environment as opposed to studies in isolation from other protein domains. Conversely, it is likely that conformational studies of whole proteins using FP fusion proteins may be affected by the presence of the fusion partners.

Calcium-Bound Structure of C-BR(L)-Y and C-BR(S)-Y. The dimensions obtained by FRET for C-BR(S)-Y in its Ca^{2+}-bound form correspond well to a conformation in which the RTX domain has adopted a 4.5-turn β roll conformation

(Table 1). The dimension for C-BR(L)-Y on the other hand is only slightly longer, suggesting that the flanking regions form a compact structure. Also, as these flanking regions lack the consensus RTX sequence, it is likely that they do not form a calcium-dependent β roll structure. Addition of calcium, however, causes the C-terminal flanking region to fold as suggested by the observed increase in Trp fluorescence.

Calcium Ion Affinity of the RTX Domains. The affinity of C-BR(L)-Y for Ca^{2+} is relatively low, with apparent K_D values of 190 μM, according to FRET *E*, and 160 μM, according to Trp fluorescence (Figure 2 and Table 2). That the two independent methods produce in similar values demonstrates that they report approximately the same conformational change. The Ca^{2+} affinity of C-BR(L)-Y was observed to decrease with an increased ionic strength (Figure 3). It is likely that due to the ionic nature of the Ca^{2+}−Asp residue interaction, Na^+ ions at sufficiently high concentrations can shield this interaction and thus reduce the RTX affinity for Ca^{2+}. The BR(L) domain has previously been shown to bind approximately six to seven calcium ions using $^{45}Ca^{2+}$ and an apparent affinity in the midmicromolar range (*13*), which is consistent with our data. Furthermore, the Ca^{2+} affinity of the α-hemolysin from *E. coli* was determined to be ~110 μM (*6*). However, the entire C-terminal RTX cluster of CyaA was shown to have a slightly lower overall Ca^{2+} affinity of ~600 μM (*12*).

The low Ca^{2+} affinity of C-BR(L)-Y was also evident in the fact that chelating agents readily reversed the conformational changes (Figure 4). This low-affinity and reversible Ca^{2+} binding is in contrast to that of some other β roll-containing proteins that have a higher Ca^{2+} affinity or bind Ca^{2+} irreversibly (*45*, *46*). The low calcium affinity of β rolls has been attributed to keeping the protein unstructured in the cytosol which would facilitate secretion through the T1 channel (*4*). Also, Ca^{2+} binding usually activates the protein functions. Thus, the Ca^{2+} binding in RTX domains seems to be an allosteric safety switch to prevent activation of potentially detrimental toxin activity in the bacterial cytosol.

Cooperativity in Calcium-Induced RTX Conformational Change. The Ca^{2+}-induced conformational change had a cooperative character as shown by both FRET and Trp measurements (Figure 2 and Table 2). The structural basis for the Ca^{2+} binding cooperativity lies in the elongated structure of this linear repeat protein. According to published X-ray crystal structures of β rolls, a calcium-binding site is formed between two adjacent turns by backbone oxygens and carboxyl groups of two Asp residues. Further, each turn coordinates two adjacent Ca^{2+} ions (Figure 1A). Cooperativity arises because binding of one ion causes the formation of half of the binding site for the next ion (along the helical axis). In addition, ion binding in one side of the domain very likely strengthens the possibility for the turns on the opposite side (perpendicular to the helical axis) to form and bind an ion. Because of the extended β roll structure, the binding of each Ca^{2+} ion only increases the affinity of an adjacent binding site, and thus, the mechanism of cooperativity is probably mostly sequential in nature. The finding that the macroscopic calcium affinities near the Trp residues and across the whole protein are very similar suggests that the individual binding sites are alike, which is consistent with the repetitive structure. The higher Hill coefficient for the C-terminal side than across the whole domain, however, indicates that the cooperativity is translated to neighboring sites more efficiently at the C-terminal side. It thus seems that the C-terminal side would be more important from the point of view of folding. This could be a factor explaining why the flanking sequences have been shown to be important (*13*). In support of this view, the folding of repeat proteins has often been observed to be nucleated at one end of the protein and then to proceed directionally along the protein toward the other end (*47*).

Role of a Central Conserved Asp Residue in the RTX Conformational Change. Asp residues are highly conserved in the sixth position in RTX motifs and only occasionally substituted with Asn residues. To study the significance of a single Asp residue and its effect on folding cooperativity, we mutated a central Asp residue in C-BR(L)-Y and BR(L) to an Ala or Pro residue. The mutants lack the carboxyl group of the Asp residue, and furthermore, the Pro mutant is more constricted in its backbone flexibility.

Both mutations reduced the apparent Ca^{2+} affinity and cooperativity as observed by FRET and Trp fluorescence (Figure 2). However, the affinity and cooperativity of the C-terminal side were much less affected as observed with Trp fluorescence, probably because the Trp residues are distant from the mutation site. The reduction in the overall apparent Ca^{2+} affinity was very pronounced considering that only one nonapeptide repeat out of nine was mutated. The mutation creates a nonresponsive site in the protein that effectively prevents cross talk between each side of the mutation and thus reduces the cooperativity. Analysis of the same mutants without the FPs using CD spectroscopy showed that both the D/A and D/P mutants had less ability to undergo Ca^{2+}-induced conformational change when compared to the wild-type RTX domain (Figure 5). Similarly, mutating two Asp residues in a β roll domain of a bacterial lipase PML variant has been reported to significantly impair Ca^{2+} binding (*48*). It was also shown that the mutant lipase had almost entirely lost its calcium-dependent enzymatic activity.

FRET as a Tool To Study Conformational Changes in RTX Domains. The developed FP-based FRET method was successfully used to study the conformational behavior of a CyaA RTX domain. The method proved to be a valuable addition to the presently available toolbox for structural analysis of conformational changes in intrinsically disordered domains. By combining the FRET method with CD and fluorescence spectroscopy, we could study both the unstructured and structured conformations, and the dynamics of the structural change. Furthermore, the construct could also potentially be used for the engineering of protein switches using in vitro evolution techniques.

ACKNOWLEDGMENT

We thank Carol Li for technical help and Elliot Campbell for help with the stopped-flow fluorescence measurements. Dr. Ladant (Institute Pasteur, Paris, France) is thanked for providing plasmid pTRCyaA$\Delta_{1\text{-}1489}\Delta_{1682\text{-}1706}$.

SUPPORTING INFORMATION AVAILABLE

Recombinant DNA work details, estimation of the dimensions of a β roll formed by the CyaA fragment, table summarizing the used RTX domain constructs, figure of time course of rapid folding and unfolding of C-BR(L)-Y, and figure of the effect of different salts on FRET *E* and Trp fluorescence. This material is available free of charge via the Internet at http://pubs.acs.org.

REFERENCES

1. Dunker, A. K., Lawson, J. D., Brown, C. J., Williams, R. M., Romero, P., Oh, J. S., Oldfield, C. J., Campen, A. M., Ratliff, C. M., Hipps, K. W.,

Ausio, J., Nissen, M. S., Reeves, R., Kang, C., Kissinger, C. R., Bailey, R. W., Griswold, M. D., Chiu, W., Garner, E. C., and Obradovic, Z. (2001) Intrinsically disordered protein. *J. Mol. Graphics Modell. 19*, 26–59.
2. Fink, A. L. (2005) Natively unfolded proteins. *Curr. Opin. Struct. Biol. 15*, 35–41.
3. Wright, P. E., and Dyson, H. J. (2009) Linking folding and binding. *Curr. Opin. Struct. Biol. 19*, 31–38.
4. Chenal, A., Guijarro, J. I., Raynal, B., Delepierre, M., and Ladant, D. (2009) RTX calcium binding motifs are intrinsically disordered in the absence of calcium: Implication for protein secretion. *J. Biol. Chem. 284*, 1781–1789.
5. Welch, R. A. (1991) Pore-forming cytolysins of Gram-negative bacteria. *Mol. Microbiol. 5*, 521–528.
6. Ostolaza, H., Soloaga, A., and Goñi, F. M. (1995) The binding of divalent cations to *Escherichia coli* α-haemolysin. *Eur. J. Biochem. 228*, 39–44.
7. Angkawidjaja, C., You, D. J., Matsumura, H., Kuwahara, K., Koga, Y., Takano, K., and Kanaya, S. (2007) Crystal structure of a family I.3 lipase from *Pseudomonas* sp. MIS38 in a closed conformation. *FEBS Lett. 581*, 5060–5064.
8. Meier, R., Drepper, T., Svensson, V., Jaeger, K. E., and Baumann, U. (2007) A calcium-gated lid and a large β-roll sandwich are revealed by the crystal structure of extracellular lipase from *Serratia marcescens*. *J. Biol. Chem. 282*, 31477–31483.
9. Glaser, P., Sakamoto, H., Bellalou, J., Ullmann, A., and Danchin, A. (1988) Secretion of cyclolysin, the calmodulin-sensitive adenylate cyclase-haemolysin bifunctional protein of *Bordetella pertussis*. *EMBO J. 7*, 3997–4004.
10. Serra, M. D., Sutton, J. M., Höper, F., Downie, J. A., and Menestrina, G. (1999) Effects of calcium and protons on the secondary structure of the nodulation protein NodO from *Rhizobium leguminosarum* biovar *viciae*. *Biochem. Biophys. Res. Commun. 263*, 516–522.
11. Baumann, U., Wu, S., Flaherty, K. M., and McKay, D. B. (1993) Three-dimensional structure of the alkaline protease of *Pseudomonas aeruginosa*: A two-domain protein with a calcium binding parallel β roll motif. *EMBO J. 12*, 3357–3364.
12. Rose, T., Sebo, P., Bellalou, J., and Ladant, D. (1995) Interaction of calcium with *Bordetella pertussis* adenylate cyclase toxin. Characterization of multiple calcium-binding sites and calcium-induced conformational changes. *J. Biol. Chem. 270*, 26370–26376.
13. Bauche, C., Chenal, A., Knapp, O., Bodenreider, C., Benz, R., Chaffotte, A., and Ladant, D. (2006) Structural and functional characterization of an essential RTX subdomain of *Bordetella pertussis* adenylate cyclase toxin. *J. Biol. Chem. 281*, 16914–16926.
14. Dominguez, D. (2004) Calcium signalling in bacteria. *Mol. Microbiol. 54*, 291–297.
15. Bejerano, M., Nisan, I., Ludwig, A., Goebel, W., and Hanski, E. (1999) Characterization of the C-terminal domain essential for toxic activity of adenylate cyclase toxin. *Mol. Microbiol. 31*, 381–392.
16. Iwaki, M., Ullmann, A., and Sebo, P. (1995) Identification by in vitro complementation of regions required for cell-invasive activity of *Bordetella pertussis* adenylate cyclase toxin. *Mol. Microbiol. 17*, 1015–1024.
17. Blenner, M., and Banta, S. (2008) Characterization of the 4D5Flu single-chain antibody with a stimulus-responsive elastin-like peptide linker: A potential reporter of peptide linker conformation. *Protein Sci. 17*, 527–536.
18. Chockalingam, K., Blenner, M., and Banta, S. (2007) Design and application of stimulus-responsive peptide systems. *Protein Eng., Des. Sel. 20*, 155–161.
19. Ambroggio, X. I., and Kuhlman, B. (2006) Design of protein conformational switches. *Curr. Opin. Struct. Biol. 16*, 525–530.
20. Banta, S., Megeed, Z., Casali, M., Rege, K., and Yarmush, M. L. (2007) Engineering protein and peptide building blocks for nanotechnology. *J. Nanosci. Nanotechnol. 7*, 387–401.
21. Ringler, P., and Schulz, G. E. (2003) Self-assembly of proteins into designed networks. *Science 302*, 106–109.
22. Reiersen, H., and Rees, A. R. (1999) An engineered minidomain containing an elastin turn exhibits a reversible temperature-induced IgG binding. *Biochemistry 38*, 14897–14905.
23. Tsien, R. Y. (1998) The green fluorescent protein. *Annu. Rev. Biochem. 67*, 509–544.
24. Clegg, R. M. (1992) Fluorescence resonance energy transfer and nucleic acids. *Methods Enzymol. 211*, 353–388.
25. Szilvay, G. R., Nakari-Setälä, T., and Linder, M. B. (2006) Behavior of *Trichoderma reesei* hydrophobins in solution: Interactions, dynamics, and multimer formation. *Biochemistry 45*, 8590–8598.
26. Patterson, G. H., Piston, D. W., and Barisas, B. G. (2000) Förster distances between green fluorescent protein pairs. *Anal. Biochem. 284*, 438–440.
27. Zhou, H. X. (2004) Polymer models of protein stability, folding, and interactions. *Biochemistry 43*, 2141–2154.
28. Jones, R. A. L. (2002) Soft condensed matter , Oxford University Press, Oxford, U.K.
29. Sreerama, N., and Woody, R. W. (1994) Protein secondary structure from circular dichroism spectroscopy. Combining variable selection principle and cluster analysis with neural network, ridge regression and self-consistent methods. *J. Mol. Biol. 242*, 497–507.
30. Ohashi, T., Galiacy, S. D., Briscoe, G., and Erickson, H. P. (2007) An experimental study of GFP-based FRET, with application to intrinsically unstructured proteins. *Protein Sci. 16*, 1429–1438.
31. Evers, T. H., van Dongen, E. M., Faesen, A. C., Meijer, E. W., and Merkx, M. (2006) Quantitative understanding of the energy transfer between fluorescent proteins connected via flexible peptide linkers. *Biochemistry 45*, 13183–13192.
32. Wielgus-Kutrowska, B., Narczyk, M., Buszko, A., Bzowska, A., and Clark, P. (2007) Folding and unfolding of a non-fluorescent mutant of green fluorescent protein. *J. Phys.: Condens. Matter 19*, 285223.
33. Lakowicz, J. R. (2006) Principles of fluorescence spectroscopy , 3rd ed., Springer, New York.
34. Stryer, L., and Haugland, R. P. (1967) Energy transfer: A spectroscopic ruler. *Proc. Natl. Acad. Sci. U.S.A. 58*, 719–726.
35. Miyawaki, A., Llopis, J., Heim, R., McCaffery, J. M., Adams, J. A., Ikura, M., and Tsien, R. Y. (1997) Fluorescent indicators for Ca^{2+} based on green fluorescent proteins and calmodulin. *Nature 388*, 882–887.
36. Evers, T. H., Appelhof, M. A., de Graaf-Heuvelmans, P. T., Meijer, E. W., and Merkx, M. (2007) Ratiometric detection of Zn(II) using chelating fluorescent protein chimeras. *J. Mol. Biol. 374*, 411–425.
37. Miyawaki, A., and Tsien, R. Y. (2000) Monitoring protein conformations and interactions by fluorescence resonance energy transfer between mutants of green fluorescent protein. *Methods Enzymol. 327*, 472–500.
38. van Dongen, E. M., Evers, T. H., Dekkers, L. M., Meijer, E. W., Klomp, L. W., and Merkx, M. (2007) Variation of linker length in ratiometric fluorescent sensor proteins allows rational tuning of Zn(II) affinity in the picomolar to femtomolar range. *J. Am. Chem. Soc. 129*, 3494–3495.
39. Lee, J. C., Langen, R., Hummel, P. A., Gray, H. B., and Winkler, J. R. (2004) α-Synuclein structures from fluorescence energy-transfer kinetics: Implications for the role of the protein in Parkinson's disease. *Proc. Natl. Acad. Sci. U.S.A. 101*, 16466–16471.
40. Uversky, V. N., Gillespie, J. R., and Fink, A. L. (2000) Why are "natively unfolded" proteins unstructured under physiologic conditions? *Proteins 41*, 415–427.
41. Binz, H., Stumpp, M., Forrer, P., Amstutz, P., and Plückthun, A. (2003) Designing repeat proteins: Well-expressed, soluble and stable proteins from combinatorial libraries of consensus ankyrin repeat proteins. *J. Mol. Biol. 332*, 489–503.
42. Main, E. R., Xiong, Y., Cocco, M. J., D'Andrea, L., and Regan, L. (2003) Design of stable α-helical arrays from an idealized TPR motif. *Structure 11*, 497–508.
43. Stumpp, M., Forrer, P., Binz, H., and Plückthun, A. (2003) Designing repeat proteins: Modular leucine-rich repeat protein libraries based on the mammalian ribonuclease inhibitor family. *J. Mol. Biol. 332*, 471–487.
44. Kapust, R. B., and Waugh, D. S. (1999) *Escherichia coli* maltose-binding protein is uncommonly effective at promoting the solubility of polypeptides to which it is fused. *Protein Sci. 8*, 1668–1674.
45. Lilie, H., Haehnel, W., Rudolph, R., and Baumann, U. (2000) Folding of a synthetic parallel β-roll protein. *FEBS Lett. 470*, 173–177.
46. Kwon, H. J., Haruki, M., Morikawa, M., Omori, K., and Kanaya, S. (2002) Role of repetitive nine-residue sequence motifs in secretion, enzymatic activity, and protein conformation of a family I.3 lipase. *J. Biosci. Bioeng. 93*, 157–164.
47. Courtemanche, N., and Barrick, D. (2008) The leucine-rich repeat domain of Internalin B folds along a polarized N-terminal pathway. *Structure 16*, 705–714.
48. Angkawidjaja, C., Paul, A., Koga, Y., Takano, K., and Kanaya, S. (2005) Importance of a repetitive nine-residue sequence motif for intracellular stability and functional structure of a family I.3 lipase. *FEBS Lett. 579*, 4707–4712.
49. Baumann, U. (1994) Crystal structure of the 50 kDa metallo protease from *Serratia marcescens*. *J. Mol. Biol. 242*, 244–251.